

Determination of Domain Sizes in Blends of Poly(ethylene) and Poly(styrene) Formed in the Presence of Supercritical Carbon Dioxide

Kristofer J. Thurecht,^{†,‡} David J. T. Hill,[‡] Christopher M. L. Preston,[‡]
Llew Rintoul,[§] John W. White,[‡] and Andrew K. Whittaker^{*,†}

Centre for Magnetic Resonance and Department of Chemistry, University of Queensland; School of Engineering, RMIT University; School of Physical Sciences, Queensland University of Technology; and Research School of Chemistry, Australian National University

Received April 16, 2004; Revised Manuscript Received May 23, 2004

ABSTRACT: Well-mixed blends of poly(ethylene) and poly(styrene) have been synthesized using supercritical carbon dioxide as a solvent. The morphology of the blends has been conclusively characterized using differential scanning calorimetry (DSC), small-angle X-ray scattering (SAXS), Raman microprobe microscopy, and ¹³C solid-state cross-polarization magic angle spinning NMR (¹³C CPMAS NMR). DSC measurements demonstrate that poly(styrene) in the blends resides solely in the amorphous regions of the poly(ethylene) matrix; however, corroborative evidence from the SAXS experiments shows that poly(styrene) resides within the interlamellar spaces. The existence of nanometer-sized domains of poly(styrene) was shown within a blend of poly(styrene) and poly(ethylene) when formed in supercritical carbon dioxide using Raman microprobe microscopy and ¹³C CPMAS NMR spectroscopy coupled with a spin diffusion model. This contrasts with blends formed at ambient pressure in the absence of solvent, in which domains of poly(styrene) in the micrometer size range are formed. This apparent improved miscibility of the two components was attributed to better penetration of the monomer prior to polymerization and increased swelling of the polymer substrate by the supercritical carbon dioxide solvent.

Introduction

The use of supercritical fluids (SCFs) in the formation of polymer blends has received intense interest over the past decade. Numerous researchers have synthesized polymeric blends through use of a SCF, generally supercritical carbon dioxide (sc-CO₂), as both a swelling agent and a solvent for vinylic monomers.^{1–6} McCarthy and Watkins¹ originally reported the use of sc-CO₂ as a solvent, and as a swelling agent, for the infusion of a monomer into a polymeric substrate. This work was based upon the initial work of Berens et al.⁷ and Sand,⁸ whereby organic penetrants were infused into poly(carbonate) and fragrances into thermoplastics, respectively. The process leading to the formation of blends involves the dissolution of the penetrant into carbon dioxide, followed by a period of infusion, and then polymerization of the penetrant usually via thermal decomposition of an initiator.

It has been shown that many polymers can be swollen considerably and in a controlled manner by SCFs. This is achieved through the manipulation of the density of the SCF by careful control of pressure and temperature. Similarly, SCFs can also expedite the diffusion of small molecules into polymer substrates. Berens et al.⁹ showed that the rate of diffusion of dimethyl phthalate into poly(vinyl chloride) could be up to 6 orders of magnitude faster if the substrate was swollen by sc-CO₂ compared to a nonswollen film. Such large increases in diffusivity upon swelling and plasticization by SCFs are not often reported in the literature; however, an increase in the order of magnitude by 1 or 2 is generally observed.¹ In

this way, Muth et al.⁶ showed that the use of sc-CO₂ as a solvent enhanced the rate of diffusion of vinylic monomers into rigid polymeric substrates but that an improvement in the compatibility between the substrate and monomer was not necessarily achieved.

When two nonpolar polymers are mixed, miscibility is rarely achieved. This is because the sum of the dispersion forces between the two polymers is smaller than the sum of the dispersion forces within each homopolymer. Specifically, the free energy term in Gibbs' equation, $\Delta G_m = \Delta H_m - T\Delta S_m$, needs to be negative, and the system must be beyond the stability limit of the spinodal¹⁰ for miscibility to be thermodynamically favorable. Since poly(ethylene) and poly(styrene) are essentially nonpolar or weakly polar, then the dominant interactions between the polymers are the weak dispersion forces.¹¹ This leads to a positive ΔH_m and necessitates a significant entropic term upon mixing for miscibility to be realized in the blends. For blends of nonpolar high molecular weight polymers the entropic term in Gibbs' equation is often not large enough to counteract this positive enthalpic term. In normal circumstances for poly(ethylene)-rich blends with poly(styrene), discrete regions of the minor component will be formed within the matrix of the major poly(ethylene) component.

The ability to measure the phase separation in polymers depends on not only the degree of phase separation but also the method which is used to probe the miscibility. Numerous methods have been used to probe the extent of mixing in a polymer blend. This is outlined in the work of Gedde,¹² who explains, for example, that light scattering experiments with micrometer resolution may suggest miscibility of mixed polymers while FT-IR, with nanometer resolution, might lead to the conclusion that two polymers do not mix well.

[†] Centre for Magnetic Resonance, University of Queensland.

[‡] Department of Chemistry, University of Queensland.

[§] Queensland University of Technology.

[‡] Australian National University.

* Corresponding author: e-mail A.Whittaker@cmr.uq.edu.au; Fax + 61 7 3365 3833.

Studies of the morphology of polymer blends formed using SCFs are rare in the literature, with the exception of reports on the use of electron microscopy techniques.⁵ Hence, despite numerous researchers claiming an improvement in the mechanical properties of polymer blends formed in *sc*-CO₂,⁵ little quantitative information has been provided of the domain sizes within these blends and of physical interactions which occur between the components of the blends.

In this paper we report a detailed analysis of the phase structure of blends of poly(ethylene) and poly(styrene) formed in the presence of the solvent *sc*-CO₂. Specifically, we report measurements of the sizes of domains of poly(styrene) following infusion and polymerization within a poly(ethylene) substrate. When mixed under normal conditions, poly(ethylene) and poly(styrene) are incompatible, forming grossly phase-separated blends. Part of this study has involved forming blends at ambient pressure for comparison with the blends formed in *sc*-CO₂. The methods of analysis used in this paper include Raman microprobe spectroscopy, ¹³C solid-state magic angle spinning nuclear magnetic resonance spectroscopy (¹³C MAS NMR), small-angle X-ray scattering (SAXS), and differential scanning calorimetry (DSC). These techniques were used to determine the extent of phase separation within the blends and the effect of blending on the morphology of the substrate.

Experimental Section

Materials. Linear low-density poly(ethylene) (LLDPE Dow 2056) was obtained from Dow Chemicals and processed as received. LLDPE 2056 has average values of M_w and M_n of 110 000 and 26 000, respectively, and contains 15.6 C6 branches per 1000 main-chain carbon atoms.¹³ The degree of crystallinity was initially 33% as determined by DSC, as described below. Styrene monomer was obtained from Sigma Aldrich and was purified by initially passing it through an Al₂O₃ column to remove the *tert*-butylcatechol inhibitor, followed by distillation in a microdistillation system under vacuum. The monomer was then stored at -4 °C away from light for up to 2 weeks. Azobis(isobutyronitrile) (AIBN) was obtained from Sigma Aldrich, recrystallized three times from methanol, and stored at -4 °C away from light.

Preparation of Film and Blends. LLDPE pellets were pressed in a hot press for 5 min at 190 °C under an applied pressure of 10 ton. The resulting sheets were approximately 10 × 5 × 0.1 cm³ in dimension. The sheets were washed in ethanol to remove any processing impurities and then cut into strips with dimensions of approximately 0.5 × 5 × 0.1 cm³.

The polymer blends were prepared using a procedure similar to that described by Muth et al.⁶ In this procedure, the films were placed in the reaction vessel with 30 vol % styrene + 1 mol % AIBN initiator. The reaction vessel, containing the poly(ethylene) substrate, styrene, and AIBN, was placed in a 40 °C water bath and allowed to come to equilibrium. The system was then purged with CO₂ and the pressure increased to the desired pressure (generally 150 bar). After an initial soaking of various time periods up to 24 h, the vessel was vented and purged three times to remove excess styrene. The styrene was polymerized within the poly(ethylene) matrix by heating of the vessel to 80 °C while maintaining the pressure of the vessel at 90 bar. Following polymerization for 4 h at the elevated temperature, the sample was weighed. Control experiments were performed at ambient pressure and 40 °C, allowing the styrene monomer and AIBN to soak into the poly(ethylene) substrate without the assistance of any solvent. Following the desired soaking period, polymerization was induced at 80 °C in a closed vessel.

Analysis. Raman microprobe spectroscopy was undertaken on a Renishaw System 1000 Raman microprobe spectrometer

equipped with a He-Ne laser operating at 632.8 nm. The microscope was an Olympus MD Plan microscope with a 50× objective lens giving a focus spot size of approximately 1 μm. Images were collected using 1 μm steps through the cross section of a precut polymer sample which had been securely mounted on the microscope stage.

Differential scanning calorimetry experiments were performed on a Perkin-Elmer DSC7 with a TAC7 computer interface. The DSC was coupled to a Windows-based software program for the analysis of the results. The instrument was calibrated using known standards: indium (T_m = 165.8 °C) and zinc (T_m = 419.5 °C). The sample, typically 2–6 mg of finely chopped polymer, was packed into aluminum DSC sample pans with the lid tightly crimped. All endotherms were baseline corrected by comparison with two scans of empty pans. The endotherms were for the first heating of the blends.

¹³C solid-state MAS NMR experiments were run on an MSL 300 spectrometer operating at 75.46 MHz for ¹³C. Samples were spun in 4 mm MAS probes at spinning speeds of up to 8 kHz. ¹³C spectra were collected via cross-polarization using a cross-polarization contact time of 1 ms. The 90° pulse time for ¹H and ¹³C nuclei was 5 μs. Values of ¹H $T_{1\rho}$ relaxation times were determined from the decay of magnetization during a spin-locking period prior to cross-polarization to the ¹³C nuclei.

Small-angle X-ray scattering measurements were performed in the Research School of Chemistry at the Australian National University using SAXS camera which is described elsewhere.¹⁴ This is a focusing Huxley-Holmes geometry with copper Kα β radiation at a wavelength of 1.54 Å. Detection is with a one-dimensional position-sensitive gas detector at 1 m from the scattering sample. In the current experiments the minimum Q was set at 0.015 Å⁻¹. (Q is the momentum transfer whose modulus $Q = 4\pi \sin \theta/\lambda$, where θ is the scattering angle, and λ is the X-ray wavelength.)

The samples were 1 mm thick taken directly from the experimental preparation and had a transmission for the X-rays of between 63% and 73% so multiple scattering was low. The data were corrected for detector sensitivity and corrected to an absolute scale (cm⁻¹) using a 1 mm water standard.

Results and Discussion

Diffusion of Styrene in Poly(ethylene). A number of previous studies have reported the characterization of the kinetics of diffusion of monomers into a polymeric substrate by measurement of the increase in weight during the sorption process. For example, Li and Han¹⁵ have investigated the effect of pressure on the maximum monomer uptake for styrene diffusing into low-density poly(ethylene). Contrary to expectations, Li and Han¹⁵ showed that a limiting pressure was reached beyond which any further increase in pressure would result in less poly(styrene) being incorporated into the final blend. This phenomenon was attributed to the competition between the increasing solvent power of the *sc*-CO₂ with increasing pressure (which tends to reduce the mass uptake) and the greater ability of *sc*-CO₂ to swell the poly(ethylene) substrate as the pressure increases (which makes the system more amenable to a higher mass uptake). Consequently, the blending experiments reported in this work were undertaken at a pressure of 150 bar, close to the optimum pressure determined by Li and Han.¹⁵

Figure 1 shows the increase in weight of LLDPE exposed to styrene monomer within *sc*-CO₂ at a pressure of 150 bar at a temperature of 45 °C. Figure 1 also shows the increase in weight of LLDPE during soaking in pure styrene at atmospheric pressure and 45 °C. After both sorption experiments the styrene was polymerized at 80 °C. A direct comparison of the two systems is shown, and a number of differences are observed.

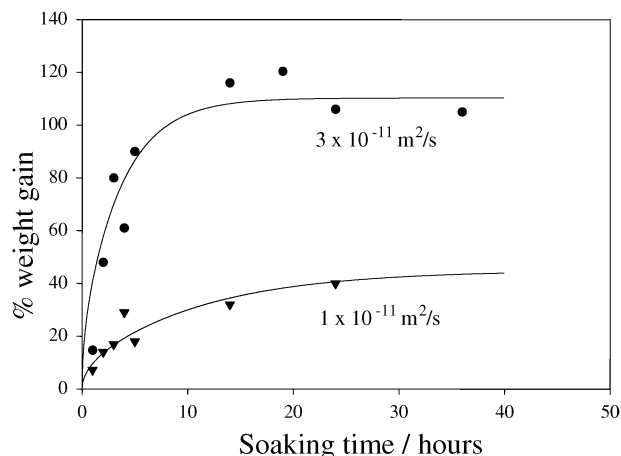


Figure 1. Mass uptake data for blend formed in supercritical CO₂ (circles) with a soaking pressure of 150 bar and blends formed at ambient pressure (triangles) in the absence of solvent. Solid curves are fits based on Fick's second law, and the calculated diffusion coefficient for each curve is included in the figure.

From Figure 1 we can see that the blend formed in the presence of sc-CO₂ as a solvent contains approximately three times the poly(styrene) of the blend formed under ambient pressure and 45 °C. This is likely due to the enhanced swelling induced by the supercritical solvent. In a parallel study,¹⁶ we have shown that sc-CO₂ penetrates and swells most polymers including poly(olefin)s and have measured increases in volumes of amorphous polymers using NMR imaging. We were unable to detect increases in volume on exposure of LLDPE to sc-CO₂ using this technique. However, measurements of ¹H NMR *T*₂ relaxation times of this polymer as a function of pressure showed that the polymer chains within the amorphous phase experienced significantly enhanced degrees of motional freedom.¹⁶ Therefore, it appears likely that the higher poly(styrene) content in the blend formed in sc-CO₂ is a result of increased free volume within the poly(ethylene) substrate.

In addition to an increased total amount of poly(styrene) formed with the blend, the data in Figure 1 show that the rate of incorporation of styrene into the LLDPE sheets is enhanced in the presence of supercritical CO₂. The maximum PSTY loading is achieved after approximately 15 h of soaking in sc-CO₂ compared with 30 h or more at ambient pressure. It has been shown previously that at the temperature and pressure used in this experiment styrene monomer and carbon dioxide exist as a single phase.¹⁷ In this way, not only does the sc-CO₂ increase the potential free volume within the poly(ethylene) substrate through swelling, but it also imparts greater diffusivity to the styrene monomer. The data in Figure 1 were fitted to the Fick's second law for diffusion of a penetrant into a planar sheet (eq 1),¹⁸ and the result of the best fit is shown as the solid line in Figure 1. The calculated diffusion coefficients are shown on the figure. In eq 1, *M_t* and *M_∞* are the masses of the blend at time *t* and at infinite time, *D* is the diffusion coefficient of the styrene monomer, and *l* is the thickness of the polymer sheet.

$$\frac{M_t}{M_\infty} = 1 - \frac{8}{\pi^2} \sum_{n=0}^{\infty} \frac{1}{(2n+1)^2} e^{-D(2n+1)^2 \pi^2 t / l^2} \quad (1)$$

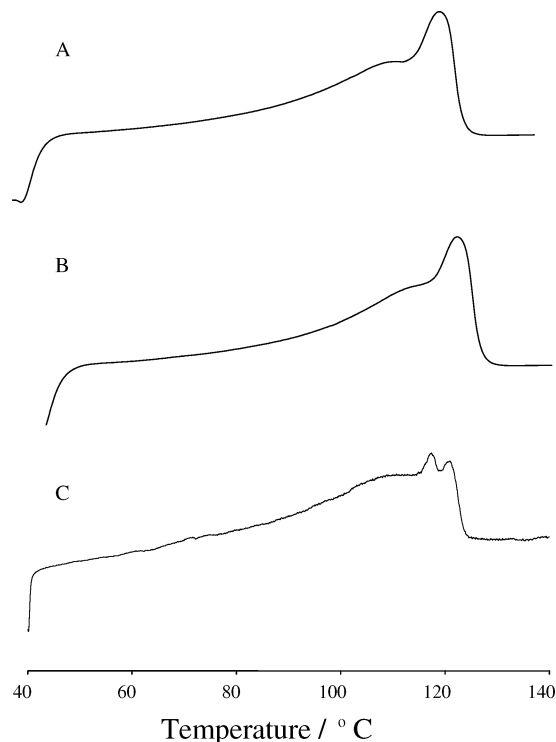


Figure 2. DSC endotherms for virgin LLDPE (A), LLDPE following swelling in sc-CO₂ for 12 h (B), and a blend of poly(ethylene) and poly(styrene) formed in sc-CO₂ at 150 bar with soaking period of 4 h (C).

The diffusion coefficient for styrene diffusing into the LLDPE substrate was determined by fitting the mass uptake data to the Fickian diffusion model. The diffusion coefficient of $3 \times 10^{-11} \text{ m}^2 \text{ s}^{-1}$ for the blend formed in the presence of sc-CO₂ compares well with values reported by other authors. Muth et al.¹⁹ measured a diffusion coefficient of $2.5 \times 10^{-11} \text{ m}^2 \text{ s}^{-1}$ for diffusion of sc-CO₂ into poly(vinyl chloride). Similarly, Kung et al.⁵ measured the diffusion of ethylbenzene into and out of high-density poly(ethylene) and determined a diffusion coefficient of $9.23 \times 10^{-11} \text{ m}^2 \text{ s}^{-1}$. In this case, the ethylbenzene was used as a nonpolymerizing model for styrene diffusion. The larger diffusion coefficient may be ascribed to the higher pressure of 240 bar being used by these authors.

Effect of Blending on Crystallinity. The incorporation of up to 120 wt % poly(styrene) into the LLDPE films is likely to result in disruption of the crystalline chain packing of the poly(olefin). The melting endotherms determined using DSC for the LLDPE sheets and the blends are shown in Figure 2. The DSC endotherm of LLDPE (Figure 2A) shows two main melting peaks with a long tail to lower temperatures. The main melting transition peak is observed at 120 °C. This is the characteristic peak of the semiordered LLDPE. The minor peak observed at 116 °C is associated with high molecular weight fractions with a low degree of branching.²⁰ The low-temperature tail of the melting endotherm is attributed to smaller and less-perfect crystals, resulting from the relatively high level of branching in this material.²⁰ The degree of crystallinity of the LLDPE sample prior to blending was found to be 33%, determined by comparison of the enthalpy of melting for the sample to that of a 100% crystalline material (292.65 J g⁻¹).¹

To determine the effect of sc-CO₂ and swelling on LLDPE, pure LLDPE was swollen in sc-CO₂ (absence of styrene monomer) for 24 h at 150 bar and 45 °C. The sample was vented slowly and the melting endotherm measured using DSC (Figure 2B). We can see from Figure 2 that there is little difference between the endotherms for the virgin poly(ethylene) and poly(ethylene) swollen in sc-CO₂. The crystalline content was determined to be 33%, identical to the starting material. The DSC results suggest that the application of high-pressure CO₂ to the material does not result in volume changes within the polymer sufficient to substantially disrupt the crystalline packing of the polymer.

The DSC trace for the LLDPE–PSTY blend formed in the presence of sc-CO₂ is shown in Figure 2C. This trace shows the two main melting peaks as observed for the original resin (Figure 2A); however, melting in the low-temperature region is significantly more pronounced. This is likely due to disruption of the crystalline order and formation of smaller crystallites by incorporation of the poly(styrene) domains into the LLDPE matrix. Despite an overall decrease in crystal size, an analysis of the enthalpy of melting of the LLDPE in this blend shows that the degree of crystallinity is not significantly altered in the blending process. This suggests that the poly(styrene) resides solely in the amorphous domains of the poly(ethylene). The poly(styrene) acts to disrupt the crystalline structure of the poly(ethylene) lamellae, as has been observed by other authors.¹ The DSC trace for the blend formed at atmospheric pressure (not shown) was very similar to that for the blend formed in sc-CO₂. This suggests that the styrene is diffusing into the amorphous regions of the LLDPE regardless of whether the polymer is swollen by the supercritical fluid or not. The glass transition temperatures of the two polymer could not be determined using DSC since that of PSTY is expected to lie below the melting endotherm of LLDPE while that of the amorphous phase of LLDPE could not be resolved from DSC measurements at low temperature. Changes in the glass transition temperatures of the two homopolymers are not expected since, as we report below, the NMR measurements confirm a degree of phase separation of the two homopolymers.

Small-Angle X-ray Scattering Studies of LLDPE–PSTY Blends. The effect of blending with poly(styrene) on the poly(ethylene) matrix was studied by small-angle X-ray scattering (SAXS). Comprehensive studies of the morphology of poly(ethylene) materials have previously appeared in the literature.^{21–23} It has been well established that the crystalline regions of poly(ethylene) generally adopt a “sheetlike” lamellar morphology with respect to the amorphous regions, the size of each region dependent on the branching length, uniformity and density,²³ as well as the thermal or processing history of the polymer.

SAXS experiments were performed on original pressed LLDPE sheets and the two blends formed either in the presence of sc-CO₂ at 150 bar or at atmospheric pressure in pure styrene. Scattering plots for the original pressed LLDPE sample and that from the blend formed in the presence of sc-CO₂ at 150 bar are shown in Figure 3. The scattering function from the blend formed at atmospheric pressure was only slightly different from that for LLDPE. A log(intensity)–log Q scale has been used to display the data because of the large dynamical range of the scattering. The large rise in scattering,

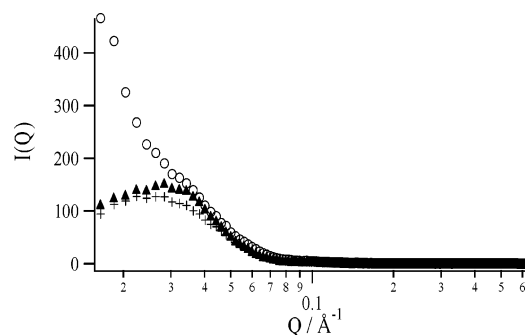


Figure 3. $I(Q)$ vs $\log(Q)$ SAX scattering data for virgin poly(ethylene) (crosses), a blend formed at ambient pressure (filled triangles), and a blend formed in sc-CO₂ (unfilled circles).

peaking near 0.03 \AA^{-1} (ca. 209 \AA Bragg spacing) for all samples, is that due to the crystalline lamellae. This scattering has been observed by other researchers for crystalline poly(ethylene).²¹

For the blend formed in sc-CO₂, greatly enhanced scattering is also observed at lower scattering angles ($Q < 0.03 \text{ \AA}^{-1}$). This enhanced scattering is not evident for the virgin poly(ethylene) or the blend formed at ambient pressure. This second population is consistent with the generation of small-angle scattering from extensive disruption of the crystalline lamellae upon incorporation of poly(styrene) into the polymer blends. This result is in agreement with the DSC results in which we observed imperfections in the poly(ethylene) crystallites in the blends formed in sc-CO₂.

Measurement of Domain Sizes Using Raman Microscopy and Solid-State NMR. It is well-known that blending of the two incompatible polymers, poly(styrene) and poly(ethylene), without the addition of compatibilizer, leads to immiscible blends,²⁴ often grossly phase separated. Materials formed with such morphology generally have inferior mechanical properties compared to well-mixed blends. In this work we therefore endeavored to measure the size of the domains of poly(styrene) within the LLDPE matrix. Raman microprobe microscopy is capable of measuring domain sizes down to a size of approximately 2 \mu m . Mixing on a much finer level can be confirmed by analysis of the decay of ¹H NMR magnetization during a ¹H $T_{1\rho}$ experiment. Measurement of NMR spin diffusion is now well established as a sensitive method for determining the sizes of discrete phases within heterogeneous polymers.^{25–27}

Raman microprobe microscopy has a spatial resolution of approximately 2 \mu m ²⁸ and so is a convenient method for studying phase-separated blends containing relatively large poly(styrene) domains. Single-point Raman spectra were collected for pure LLDPE, pure poly(styrene), and a blend of LLDPE and poly(styrene) (Figure 4). The mapping technique allows mapping of the cross section of the blends (Figure 5) to provide a two-dimensional profile of the concentration of poly(styrene) throughout the LLDPE substrate. In addition, area mapping was used to determine the poly(styrene) concentration in the sample (Figure 6) along a cross section. The Raman technique can only be used to determine concentrations of poly(styrene) if well-separated peaks can be resolved due to both the poly(styrene) and poly(ethylene) components in the blends. The peaks in the Raman spectrum at 1000 and 1300 cm^{-1} were used for analysis. These were assigned to the carbon–carbon stretching band of poly(styrene)^{28,29} and the CH₂ twisting band of amorphous poly(ethylene),³⁰

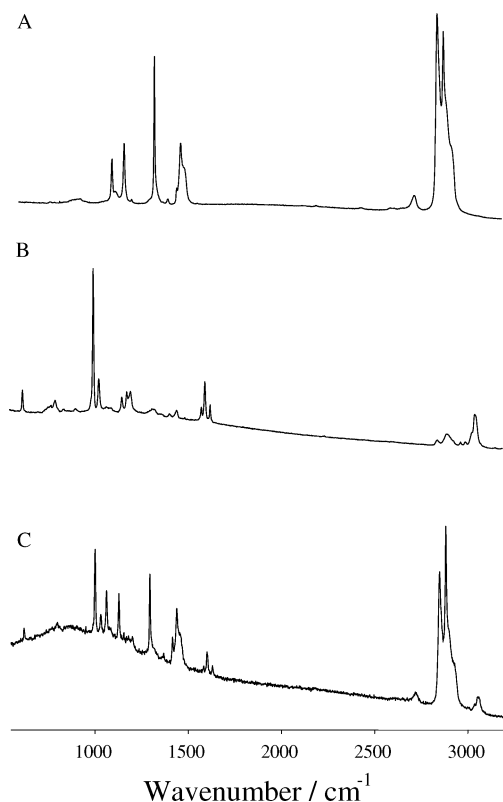


Figure 4. Raman spectra of poly(ethylene) (A), poly(styrene) (B), and a blend of poly(ethylene) and poly(styrene) (C).

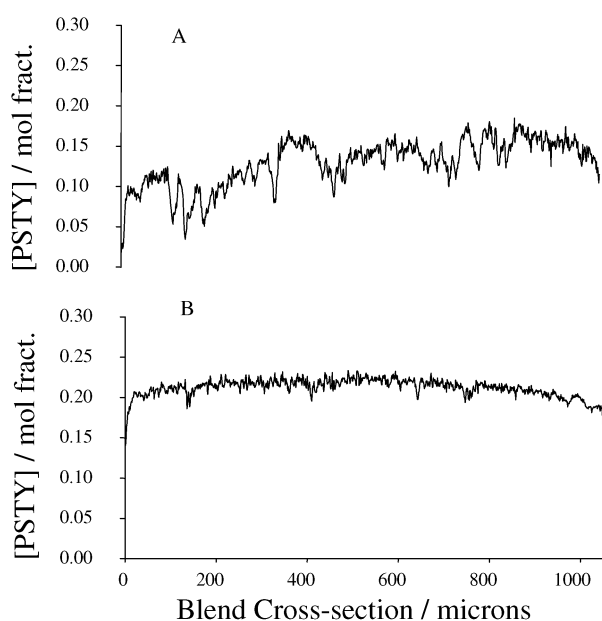


Figure 5. Raman line map of the poly(styrene) concentration across a blend formed at ambient pressure (A) and a blend formed in sc-CO₂ (B).

respectively. Other assignments are given in Table 1.

It is possible to attain semiquantitative measurements of absolute concentrations of the components of the blends within the area or the line maps by normalizing the spectra with the Raman cross section (ϕ) from the pure homopolymers, as described by eq 2:

$$\chi_{\text{psty}} = (I_{\text{psty}}/\phi_{\text{psty}})/[(I_{\text{psty}}/\phi_{\text{psty}}) + (I_{\text{pe}}/\phi_{\text{pe}})] \quad (2)$$

where χ_{psty} is the mole fraction of poly(styrene), I_{psty} and

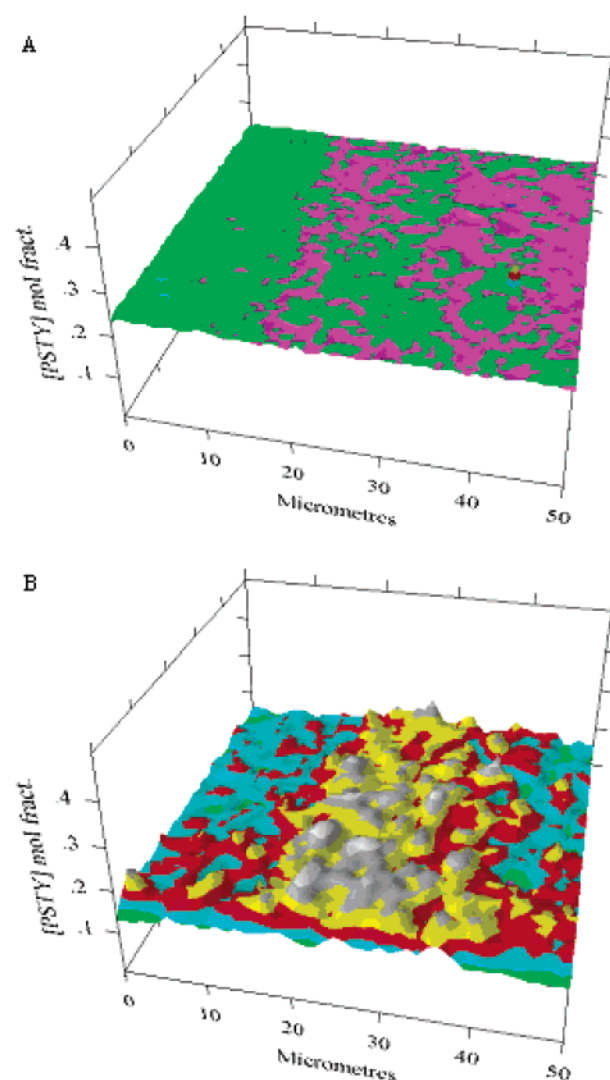


Figure 6. Raman maps of a surface through the cross section of a blend formed in sc-CO₂ (A) and at ambient pressure (B). Z-axis is concentration of poly(styrene).

Table 1. Assignment of Raman Bands Observed in Blends of Poly(ethylene) and Poly(styrene)^{24,25}

wavenumber	assignment	polymer
996	C—C stretch	PSTY
1034	C—H in-plane bending	PSTY
1054	C—H in-plane bending	PSTY
1059	C—C stretch	PE
1125	C—H in-plane bending	PSTY
1132	C—C stretch	PE
1184	C—H in-plane bending	PSTY
1296	CH ₂ twisting	PE
1442	CH ₂ bending	PE
1579	C—C stretch	PSTY
1600	C—C stretch	PSTY
1629	C=C stretch	PSTY
2850	aliphatic C—H stretch	PE
2884	aliphatic C—H stretch	PE
2900	aliphatic C—H stretch	PSTY
3050	aromatic C—H stretch	PSTY

I_{pe} are the intensities of the peaks at 1000 and 1300 cm⁻¹, respectively and ϕ_{psty} and ϕ_{pe} are the Raman cross sections of these two peaks.

It should be noted that confocal Raman microscopy is very sensitive to the focusing of the microscope, and care was taken to ensure that the whole area of interest was in focus at the time of measurement. Small dis-

crepancies in the focus can lead to sizable errors in the absolute concentrations calculated.

The Raman microprobe microscopy method was initially used to measure the distribution of poly(styrene) across the width of the blend sheet. A typical line map is shown in Figure 5 in which the normalized concentration of poly(styrene) through the cross section of a blend formed in supercritical CO₂ (Figure 5A) and at ambient pressure (Figure 5B) is plotted. In all of the materials studied, poly(styrene) was present across the whole cross section of the sheet. The apparent decrease in poly(styrene) concentration at the edges of the film is probably due to desorption of styrene monomer between the soaking period and polymerization.

The true advantage of the Raman technique is made apparent in the area mapping of the samples (Figure 6). Maps were made by recording spectra in 1 μ m steps across an area of 50 \times 50 μ m. Concentrations of PSTY were calculated using the relative peak intensities and eq 2. Figure 6 shows the Raman maps obtained for a blend formed in sc-CO₂ and a blend formed at ambient pressure. Note that the *z*-axis is a measure of PSTY concentration, not topography. In the first instance, it can be clearly seen that well-defined domains are not observed in the blend formed in sc-CO₂. The Raman maps are relatively smooth and featureless and suggest that the poly(styrene) domains in this blend are much smaller than the approximately 2 μ m spatial resolution of the microscope. The map for the blend formed at ambient pressure, however, reveals an intensity map indicative of a cross section with micron-sized domains of PSTY within the LLDPE. In this map, discrete "humps" represent dense regions of poly(styrene) which are up to 5 μ m in diameter and are dispersed evenly throughout the area of the map. This result concurs with literature reports whereby the incompatible poly(styrene) and poly(ethylene) phase separate to a large extent under normal blending conditions. Furthermore, the area maps of the blends formed in sc-CO₂ reveal that the PSTY domains are much smaller than the 2 μ m resolution of Raman microprobe spectroscopy.

¹³C CPMAS NMR has been used extensively to probe the miscibility of polymer blends.^{31–35} In particular, the rate of diffusion of ¹H magnetization through proton-rich heterogeneous blends can be analyzed, using appropriate models, to extract average domain sizes. ¹H *T*_{1ρ} relaxation times, measured by observing the decay of ¹H magnetization prior to cross-polarization to ¹³C nuclei, were evaluated for a number of polymer blends formed in sc-CO₂ and at ambient pressure. By varying the spin-locking times, from 10 μ s up to 25 ms, the relaxation behavior of the system could be determined. The ¹H *T*_{1ρ} relaxation curves were then fitted to a biexponential relaxation function. As reported by many authors including Packer and co-workers,³² the short ¹H *T*_{1ρ} relaxation time of poly(ethylene) arises from decay of magnetization of protons within the amorphous regions, while the long relaxation time is due to relaxation of the magnetization in the crystalline regions of the polymer. The protons relaxing rapidly within the amorphous region provide a "relaxation sink" for the magnetization within other regions in the polymer, provided they are coupled to each other by effective spin diffusion pathways.

The DSC results discussed above indicated that the poly(styrene) within the blends was concentrated in the amorphous regions of the poly(ethylene). The DSC

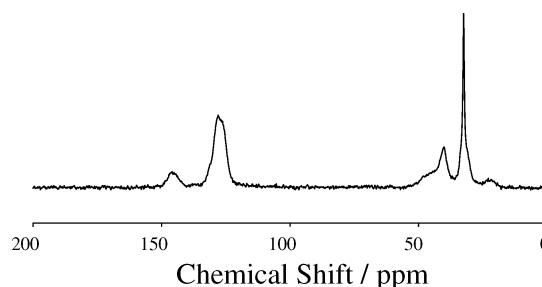


Figure 7. ¹³C CPMAS solid-state NMR spectrum of a blend of poly(ethylene) and poly(styrene).

Table 2. Assignment of NMR Peaks Observed in ¹³C CPMAS Spectra of Blends of Poly(ethylene) and Poly(styrene)^{31,32}

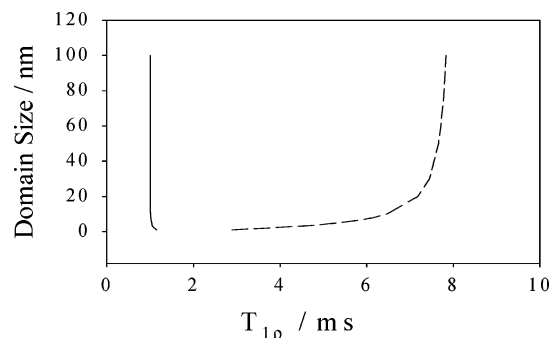
chemical shift	assignment	polymer
21	amorphous	PE
32.5	crystalline	PE
40	methine and methylene carbons	PSTY
127	protonated aromatic carbon	PSTY
145	nonprotonated aromatic carbon	PSTY

results showed that the overall crystal size decreased slightly on blending but that the total crystallinity was not reduced. Greater mixing of protons would therefore occur in the amorphous regions of the poly(ethylene) with poly(styrene). To probe this interaction, we concentrated on the effects of mixing on the short ¹H *T*_{1ρ} of poly(ethylene) upon addition of poly(styrene). Figure 7 shows a typical ¹³C MAS NMR spectrum of a blend of poly(ethylene) and poly(styrene). The assignments to the spectrum are given in Table 2.^{36,37} Relaxation times corresponding to different chemical species, resolved in the ¹³C CPMAS spectrum, were obtained by analysis of the decay of magnetization in a two-dimensional NMR experiment, in which the second dimension is the spin-locking time.

A two-region, one-dimensional lamellar model of the decay of magnetization³¹ was used to determine the poly(styrene) domain size in the samples studied. The analysis uses intrinsic ¹H *T*_{1ρ} relaxation times for amorphous poly(ethylene) and poly(styrene) of 2 and 8 ms, respectively. This model requires estimates of relative concentrations of each component and the ¹H spin diffusion coefficients with each phase.³¹ The former could be obtained from appropriate ¹³C CPMAS spectra and the latter estimated from the line widths within the broad-line ¹H NMR spectra.³⁸ Theoretical relaxation time curves were generated using these parameters for model blends with a range of values of average domain sizes, i.e., repeat distances in the lamellar model of morphology. The resultant relaxation behavior was compared with the experimentally determined relaxation behavior, and limits to the domain sizes were deduced. Figure 8 shows an example of results that we obtained considering a representative blend formed in sc-CO₂. It can be clearly seen that for small domain sizes within the model the ¹H *T*_{1ρ} relaxation times of the two phases would be effectively averaged to a single value by spin diffusion. As the size of the domains is increased, the relaxation times are expected to approach the values measured for the pure materials. Figure 8 also shows that the ¹H *T*_{1ρ} of the protons within the poly(styrene) would be expected to vary to a greater extent than the ¹H *T*_{1ρ} for the protons in amorphous poly(ethylene). Indeed, the model suggests that for poly(styrene) domains of approximately 5 nm in size the ¹H *T*_{1ρ} for poly-

Table 3. Comparison of the Values of ^1H $T_{1\rho}$ and the Corresponding Domain Sizes for a Blend Formed in sc- CO_2 and a Blend Formed at Ambient Pressure

blend	polymer	intrinsic ^1H $T_{1\rho}$ (ms)	exptl ^1H $T_{1\rho}$ (ms)	^1H $T_{1\rho}$ (ms) determined from model	calcd domain size (nm)
blend formed in sc- CO_2	LLDPE	8	4.91	4.95	4
	PSTY	1	0.6	1.04	
blend formed at 1 bar	LLDPE	8	8.2	8	>100
	PSTY	1	1.2	1	

**Figure 8.** ^1H $T_{1\rho}$ values for poly(styrene) (dashed line) and the amorphous phase of poly(ethylene) (solid line) in blends of poly(styrene) and poly(ethylene) calculated using the one-dimensional diffusion model described in the text.

(styrene) protons would decrease from 8 to 3 ms, whereas for the poly(ethylene) protons the relaxation time is predicted to increase only slightly above the initial value of 2 ms (Figure 8). The figure also demonstrates that in this system the observed values of ^1H $T_{1\rho}$ would be close to those observed for the pure homopolymers when the blend domain size was greater than approximately 100 nm.

Table 3 presents the ^1H $T_{1\rho}$ values measured using NMR for a blend formed in the presence of supercritical CO_2 and for a blend formed at ambient pressure, along with the intrinsic $T_{1\rho}$ values of the homopolymers. Clearly, and as expected, the value of ^1H $T_{1\rho}$ for poly(styrene) in the blend formed at ambient pressure was similar to the intrinsic ^1H $T_{1\rho}$ of pure poly(styrene). This suggests that the domain sizes in this particular blend are greater than 100 nm and therefore are too large to allow effective averaging of the ^1H $T_{1\rho}$ relaxation times of the two polymer components in the blend. On the other hand, the value of ^1H $T_{1\rho}$ for poly(styrene) in the blend formed in the presence of sc- CO_2 was seen to decrease considerably compared to the intrinsic value for the homopolymer. Unlike the blend formed at ambient pressure, the domain sizes in this blend are sufficiently small to the extent that averaging of the ^1H $T_{1\rho}$ of the poly(styrene) protons is observed. These results support the Raman microprobe measurements, which showed that the size of PSTY domains in the blends formed at ambient pressure are the order of microns in size—well beyond the limit at which averaging of ^1H $T_{1\rho}$ occurs. The Raman microprobe microscopy results also show that the PSTY phases within the blends formed in the presence of sc- CO_2 were much smaller than 2 μm .

The aforementioned two-region, one-dimensional lamellar model was used to estimate the domain sizes within a typical blend formed in sc- CO_2 . The observed values of ^1H $T_{1\rho}$ for the protons in amorphous poly(ethylene) and poly(styrene) regions suggest an average domain size of 4 nm for this blend. This is approximately 3 orders of magnitude smaller than the domains within the blend formed at ambient pressure as determined

by the Raman mapping. In this work many blends were formed in sc- CO_2 under various CO_2 densities. For samples with 40 wt % poly(styrene) or less, the NMR relaxation properties were consistent with poly(styrene) domains of approximately 14 nm. This is in agreement with the results of Liu et al.,³⁹ whereby improved mechanical properties are reported for blends formed using sc- CO_2 compared to conventionally blended copolymers. For example, an improvement in the tensile strength has been reported for blends formed in sc- CO_2 . This is consistent with greater compatibility between the two homopolymers in the blend.

Summary

The effect of use of sc- CO_2 as a solvent for styrene monomer on the morphology of LLDPE–PSTY polymer blends has been examined. The use of SCFs as a solvent and swelling agent leads to a much higher degree of mixing of the two polymers when compared to blending at ambient pressures. Some disruption of the crystalline structure of LLDPE is observed upon blending; however, the degree of crystallinity in the poly(ethylene)—the major component of the blend—is unaffected regardless of whether the blending was undertaken under supercritical conditions or at ambient pressure. Evidence of crystallite disruption is also observed in the ^{13}C MAS NMR spectrum by the appearance of a small peak at 35 ppm assigned to monoclinic poly(ethylene) crystals. Hence, the styrene monomer must only diffuse into the amorphous regions of the LLDPE matrix, and the amount of monomer absorbed must be sufficient to cause swelling of the matrix upon polymerization.

The domain sizes of the blends formed in sc- CO_2 and at ambient pressure contrast dramatically, with the blend formed at ambient pressure exhibiting greater phase separation than the blend formed using sc- CO_2 as a solvent. This may be explained by the swelling power of sc- CO_2 which provides greater free volume in the amorphous regions of the poly(ethylene) matrix. This allows the styrene monomer to penetrate the matrix more freely. This swelling induces greater mixing between the poly(ethylene) and poly(styrene) for the blend formed in sc- CO_2 . The close proximity of the polymer chains in the two components of the blend leads to partial averaging of the ^1H $T_{1\rho}$ NMR relaxation times. Analysis of the relaxation times leads to the conclusion that domain sizes of approximately 4 nm are being formed within blends prepared using sc- CO_2 . This contrasts with the blends formed at ambient pressure which show no mixing on the nanometer scale. On the contrary, Raman microprobe microscopy suggests that the poly(styrene) domains in these blends have sizes of the order of microns.

Acknowledgment. The authors gratefully acknowledge the financial support of the University of Queensland in supporting this work.

References and Notes

- (1) Watkins, J. J.; McCarthy, T. J. *Macromolecules* **1994**, *27*, 4845–4847.
- (2) Walker, T. A.; Raghavan, S. R.; Royer, J. R.; Smith, S. D.; Wignall, G. D.; Melnichenko, Y.; Khan, S. A.; Spontak, J. J. *Phys. Chem. B* **1999**, *103*, 5472–5476.
- (3) Li, D.; Liu, Z.; Han, B.; Song, L.; Yang, G.; Jiang, T. *Polymer* **2002**, *43*, 5363–5367.
- (4) Rajagopalan, P.; McCarthy, J. *Macromolecules* **1998**, *31*, 4791–4797.
- (5) Kung, E.; Lesser, A. J.; McCarthy, T. J. *Macromolecules* **1998**, *31*, 4160–4169.
- (6) Muth, O.; Hirth, T.; Vogel, H. *J. Supercrit. Fluids* **2000**, *17*, 65–72.
- (7) Berens, A. R.; Huvard, G. S.; Korsmeyer, R. W. Goodrich Co B F: US, 1987.
- (8) Sand, M. L. Hercules Incorporated: U.S. Patent No: 4598006, 1986.
- (9) Berens, A. R.; Huvard, G. S.; Korsmeyer, R. W.; Kunig, F. W. *J. Appl. Polym. Sci.* **1992**, *46*, 231–242.
- (10) Olabisi, O.; Robeson, L. M.; Shaw, M. T. *Polymer–Polymer Miscibility*; Academic Press: New York, 1979.
- (11) Rudin, A. In *The Elements of Polymer Science and Engineering*, 2nd ed.; Academic Press: San Diego, 1999; pp 445–496.
- (12) Gedde, U. W. *Polymer Physics*; Chapman & Hall: New York, 1995.
- (13) Bremner, T. Personal communication, 1995.
- (14) Aldissi, M.; Henderson, S. J.; White, J. L.; Zemb, T. *Mater. Sci. Forum* **1988**, *27–28*, 437–444.
- (15) Han, B.; Li, D. *Macromolecules* **2000**, *33*, 4555–4560.
- (16) Thurecht, K. J.; Whittaker, A. K.; Hill, D. J. T. *Macromolecules*, in press.
- (17) Suppes, G. J.; McHugh, M. A. *J. Chem. Eng. Data* **1989**, *34*, 310–312.
- (18) Crank, J. *The Mathematics of Diffusion*, 1st ed.; Oxford University Press: London, 1956.
- (19) Muth, O.; Vogel, H.; Hirth, T. *J. Supercrit. Fluids* **2001**, *19*, 299–306.
- (20) Schouterden, P.; Groeninckx, G.; Van der Heijden, B.; Jansen, F. *Polymer* **1987**, *28*, 2099–2104.
- (21) Wignall, G. D.; Alamo, R. G.; Londono, J. D.; Mandelkern, L.; Kim, M. H.; Lin, J. S.; Brown, G. M. *Macromolecules* **2000**, *33*, 551–561.
- (22) Mathot, V. B. F.; Scherrenberg, R. L.; Pijpers, T. F. J. *Polymer* **1998**, *39*, 4541–4559.
- (23) Marigo, A.; Marega, C.; Zannetti, R.; Sgarzi, P. *Eur. Polym. J.* **1998**, *34*, 597–603.
- (24) Favis, B. D.; Li, J. *Polymer* **2001**, *42*, 5047–5053.
- (25) Demco, D. E.; Johansson, A.; Tegenfeldt, J. *Solid State Nucl. Magn. Reson.* **1994**, *4*, 13–38.
- (26) Schmidt-Rohr, K.; Spiess, H. W. *Multidimensional Solid-State NMR and Polymers*; Academic Press: London, 1994.
- (27) VanderHart, D. L.; McFadden, G. B. *Solid State Nucl. Magn. Reson.* **1996**, *7*, 45–66.
- (28) Quintana, S. L.; Schmidt, P.; Dybal, J.; Kratochvil, J.; Pastor, J. M.; Merino, J. C. *Polymer* **2002**, *43*, 5187–5195.
- (29) Sears, W. M.; Hunt, J. L.; Stevens, J. R. *J. Chem. Phys.* **1981**, *75*, 1589.
- (30) Sato, H.; Shimoyama, M.; Kamiya, T.; Amari, T.; Sasic, S.; Ninomiya, T.; Siesler, H. W.; Ozaki, Y. *J. Appl. Polym. Sci.* **2002**, *86*, 443–448.
- (31) Cudby, M. E. A.; Packer, K. J.; Hendra, P. J. *Polym. Commun.* **1984**, *25*, 303–305.
- (32) Packer, K. J.; Pope, J. M.; Yeung, R. R.; Cudby, M. E. A. *J. Polym. Sci., Polym. Phys. Ed.* **1984**, *25*, 589–616.
- (33) Jack, K. S.; Natansohn, A.; Wang, J. *Chem. Mater.* **1998**, *10*, 1301–1308.
- (34) Wang, J. *J. Chem. Phys.* **1996**, *104*, 4850.
- (35) Whittaker, A. K. In *Polymer Characterisation Techniques and Their Application to Blends*; Simon, G., Ed.; Oxford University Press: New York, 2003; pp 461–503.
- (36) Miyoshi, T.; Takegoshi, K.; Terao, T. *Macromolecules* **1997**, *30*, 6582–6585.
- (37) Hu, G. W.; Schmidt-Rohr, K. *Polymer* **2000**, *41*, 2979–2987.
- (38) Kimura, T.; Neki, K.; Tamura, N.; Horii, F.; Nakagawa, M.; Odani, H. *Polymer* **1990**, *33*, 493–497.
- (39) Liu, Z.; Dong, Z.; Han, B.; Wang, J.; He, J.; Yang, G. *Chem. Mater.* **2002**, *14*, 4619–4623.

MA0492622